Genetic dissection of ion currents underlying all-or-none action potentials in *C. elegans* body-wall muscle cells

Ping Liu[1], Qian Ge[1], Bojun Chen[1], Lawrence Salkoff[2], Michael I. Kotlikoff[3] and Zhao-Wen Wang[1]

[1] *Department of Neuroscience, University of Connecticut Health Center, Farmington, CT, USA*
[2] *Department of Anatomy and Neurobiology, Washington University School of Medicine, St Louis, MO, USA*
[3] *College of Veterinary Medicine, Cornell University, Ithaca, NY, USA*

Non-technical summary Mammalian skeletal muscle contractions are initiated by all-or-none action potentials (APs) triggered by motoneurons. In *C. elegans* locomotory muscle, however, the characteristics of APs, the underlying ion channels, and their role in Ca^{2+} release are poorly understood. Here we show that *C. elegans* locomotory muscle fires spontaneous, all-or-none APs, which appear to be modulated by motoneuron activity. The upstroke of muscle APs requires Ca^{2+} entry through a voltage-gated Ca^{2+} channel (EGL-19), whereas the downstroke of the APs relies on a voltage-gated potassium channel as well as a Ca^{2+}- and Cl^{-}-activated potassium channel. AP-elicited elevations of intracellular Ca^{2+} concentration require both EGL-19 in the plasma membrane and the ryanodine receptor in the sarcoplasmic reticulum membrane. The discovery of all-or-none action potentials in *C. elegans* body-wall muscle brings the physiology of *C. elegans* much closer to that of other metazoans, and strengthens its utility as a model organism.

Abstract Although the neuromuscular system of *C. elegans* has been studied intensively, little is known about the properties of muscle action potentials (APs). By combining mutant analyses with *in vivo* electrophysiological recording techniques and Ca^{2+} imaging, we have established the fundamental properties and molecular determinants of body-wall muscle APs. We show that, unlike mammalian skeletal muscle APs, *C. elegans* muscle APs occur in spontaneous trains, do not require the function of postsynaptic receptors, and are all-or-none overshooting events, rather than graded potentials as has been previously reported. Furthermore, we show that muscle APs depend on Ca^{2+} entry through the L-type Ca^{2+} channel EGL-19 with a contribution from the T-type Ca^{2+} channel CCA-1. Both the *Shaker* K^{+} channel SHK-1 and the Ca^{2+}/Cl^{-}-gated K^{+} channel SLO-2 play important roles in controlling the speed of membrane repolarization, the amplitude of afterhyperpolarization (AHP) and the pattern of AP firing; SLO-2 is also important in setting the resting membrane potential. Finally, AP-elicited elevations of $[Ca^{2+}]_i$ require both EGL-19 and the ryanodine receptor UNC-68. Thus, like mammalian skeletal muscle, *C. elegans* body-wall myocytes generate all-or-none APs, which evoke Ca^{2+} release from the sarcoplasmic reticulum (SR), although the specific ion channels used for AP upstroke and repolarization differ.

(Resubmitted 9 October 2010; accepted after revision 5 November 2010; first published online 8 November 2010)
Corresponding author Z.-W. Wang: Department of Neuroscience, University of Connecticut Health Center, 263 Farmington Avenue, Farmington, CT 06030-3401, USA. Email: zwwang@uchc.edu

Abbreviations ACh, acetylcholine; AHP, afterhyperpolarization; AP, action potential; DHPR, dihydropyridine receptor; *gf*, gain-of-function; P*myo-3*, *myo-3* promoter; ROI, regions of interest; RyR, ryanodine receptor; SR, sarcoplasmic reticulum; TBC, d-tubocurarine; VGCC, voltage-gated Ca^{2+} channel.

DOI: 10.1113/jphysiol.2010.200683

Introduction

Action potentials (APs) are hallmarks of excitable cells. In mammalian skeletal muscle, Na^+-dependent APs of short duration (less than a few milliseconds) underlie excitation–contraction coupling (Cooke & Grinnell, 1964; Redfern *et al.* 1970; Cruz *et al.* 1985; Catterall, 1986; Wolters *et al.* 1994; Cairns *et al.* 2003). APs are triggered by acetylcholine (ACh)-evoked end-plate potentials, and travel into transverse tubules where they activate the dihydropyridine receptor (DHPR), which is a $Ca_V1.1$/L-type voltage-gated Ca^{2+} channel (VGCC). The activation of DHPRs causes ryanodine receptor (RyR)-mediated Ca^{2+} release from the SR through protein–protein interactions between the DHPR and RyR (Schneider, 1994) rather than Ca^{2+}-induced Ca^{2+} release, which generally occurs in cardiomyocytes (Cannell *et al.* 1995), some smooth muscle cells (Kotlikoff, 2003) and neurons (Verkhratsky & Shmigol, 1996). The SR appears to be the primary source of Ca^{2+} in skeletal muscle cells because blockade of Ca^{2+} entry does not have an obvious effect on the elevation of $[Ca^{2+}]_i$ in response to membrane depolarization (Nakai *et al.* 1996). The SCN4A/$Na_V1.4$ Na^+ channel is the major Na^+ channel expressed in innervated mammalian skeletal muscle (Trimmer *et al.* 1989), whereas the CLCN1/CLC-1 Cl^- channel dominates the resting conductance of skeletal muscle and probably plays an important role in spike repolarization (Hudson *et al.* 1995; Jentsch *et al.* 1999).

C. elegans body-wall muscle is analogous to vertebrate skeletal muscle in structure and function (Moerman & Fire, 1997; Lecroisey *et al.* 2007); however, little is known about the property of APs and the mechanism of excitation–contraction coupling of *C. elegans* body-wall muscle cells. While it has been reported that graded APs occur in *C. elegans* body-wall muscle cells (Jospin *et al.* 2002), the general properties of body-wall muscle APs, the ion channels underlying the resting membrane potential and shaping AP waveform, and the processes of Ca^{2+} release are largely unknown.

As *C. elegans* does not have genes encoding homologues of known voltage-gated Na^+ channels (Bargmann, 1998), APs in body-wall muscle cells most probably result from the activation of Ca^{2+} channels or other cation channels. Homologues of the pore-forming α_1-subunit of three different vertebrate voltage-gated Ca^{2+} channels (VGCCs) are found in *C. elegans*, including UNC-2 (Ca_V2 or N/P/Q-type), EGL-19 (Ca_V1 or L-type) and CCA-1 (Ca_V3 or T-type) (Bargmann, 1998). In addition, *C. elegans* has NCA-1 and NCA-2 (Jospin *et al.* 2007; Yeh *et al.* 2008), which are homologues of the mammalian NALCN, a voltage-independent, non-selective cation channel (Lu *et al.* 2007). NCA-1 and NCA-2 resemble the pore-forming subunit of voltage-gated Ca^{2+} or Na^+ channels in having four repeating domains with similar putative topology, but they are distinct in the primary sequence. EGL-19 and, possibly, CCA-1 are expressed in body-wall muscle cells (Lee *et al.* 1997; Steger *et al.* 2005), and EGL-19 is a major carrier of inward current, playing an important role in generating the reported graded APs in body-wall muscle cells (Jospin *et al.* 2002). The other three channels (UNC-2, NCA-1 and NCA-2) are primarily expressed in the nervous system with muscle expression detected only at the worm tail for NCA-2 (www.wormbase.org). In addition, *C. elegans* body-wall muscle cells express a variety of K^+ channels (Kunkel *et al.* 2000; Yuan *et al.* 2000; Salkoff *et al.* 2001; Wang *et al.* 2001; Salkoff *et al.* 2005) and a RyR, which is encoded by the *unc-68* gene (Maryon *et al.* 1998). Three of the identified K^+ channels, including SHL-1 (*Shal* or Kv4 type), SHK-1 (*Shaker* or Kv1 type) and SLO-2 (Ca^{2+}- and Cl^--gated) appear to be the predominant carriers of outward currents (Santi *et al.* 2003; Fawcett *et al.* 2006).

In the present study, we determined the electrical properties of APs in *C. elegans* body-wall muscle cells, analysed the role of specific ion channel gene products in generating and shaping APs, and determined how APs lead to an elevation of $[Ca^{2+}]_i$ and muscle contraction. We found that body-wall muscle APs are all-or-none events rather than graded depolarizations as previously reported, and that unlike those of mammalian skeletal muscle fibres, body-wall muscle APs occur in the absence of neural input. We also report that SHK-1 and SLO-2 K^+ channels contribute to body-wall muscle APs, and that trains of APs are associated with elevations of $[Ca^{2+}]_i$, which required the functions of both the EGL-19 Ca^{2+} channel and the UNC-68 ryanodine receptor channel.

Methods

Culturing of *C. elegans*

Worms were grown inside an incubator (21°C) on agar plates with a layer of OP50 *Escherichia coli* (Sulston & Hodgkin, 1988).

Recording of membrane potentials and currents

Adult hermaphrodite animals were immobilized and dissected as described previously (Wang *et al.* 2001; Liu *et al.* 2005). Briefly, an animal was immobilized on a glass coverslip by applying 3M Vetbond Tissue Adhesive (3M Company, MN, USA) along the dorsal side. Application of the adhesive was generally restricted to the middle portion of the animal, which allowed movements of the head and tail during the experiment. A longitudinal incision was made in the dorsolateral region. After clearing the viscera, the cuticle flap was folded back and glued to the coverslip, exposing the ventral nerve cord and the two adjacent muscle quadrants. A Nikon FN-1 microscope equipped

with a 40× water-immersion objective and 15× eyepieces was used for viewing the preparation. Borosilicate glass pipettes with a tip resistance of 3∼5 MΩ were used as electrodes for current- and voltage-clamp recordings in the classical whole-cell patch-clamp configuration. Current- and voltage-clamp experiments were performed with a Multiclamp 700B amplifier (Molecular Devices, Sunnyvale, CA, USA) and the Clampex software (version 10, Molecular Devices). Data were sampled at a rate of 10 kHz after filtering at 2 kHz.

All the current-clamp experiments, except when specified otherwise, were performed without current injection. The holding potential was −60 mV in all voltage-clamp experiments. Outward currents were recorded by applying 1200 ms voltage steps from −60 to +70 mV at 10 mV intervals whereas inward currents were recorded by applying 200 ms voltage steps from −40 to +60 mV at 10 mV intervals. In experiments recording membrane potential changes and whole-cell outward current, the standard bath solution contained (in mM): NaCl 140, KCl 5, $CaCl_2$ 5, $MgCl_2$ 5, dextrose 11 and HEPES 5 (pH 7.2, 320 mOsm); and the standard pipette solution contained (in mM): KCl 120, KOH 20, Tris 5, $CaCl_2$ 0.25, $MgCl_2$ 4, sucrose 36, EGTA 5 and Na_2ATP 4 (pH 7.2, 323 mOsm). In experiments recording whole-cell inward current, the standard bath solution contained (in mM): NaCl 120, KCl 5, $CaCl_2$ 5, $MgCl_2$ 5, dextrose 11, HEPES 5, tetraethylammonium chloride (TEACl) 20, and 4-aminopyridine 3 (pH 7.2, 323 mOsm); and the standard pipette solution contained (in mM): CsCl 140, MgATP 4, TEACl 5, EGTA 5, and Tris 5 (pH 7.2, 296 mOsm).

Imaging muscle Ca^{2+} transients

GCaMP2 (Tallini *et al.* 2006) was synthesized with codon optimization and introduction of two introns for improved expression in *C. elegans*. The synthesized GCaMP2 was cloned into a vector containing the *myo-3* myosin promoter (P*myo-3*) (Okkema *et al.* 1993), and expressed in worms through a transgenic injection. Integrated transgenic worms (zw495 strain) expressing the P*myo-3*::GCaMP2 (wp962) were obtained following standard procedures (Evans, 2006), backcrossed 3 times with the wild-type, and subsequently crossed into the *unc-68(r1162)* strain (Maryon *et al.* 1996). Spontaneous $[Ca^{2+}]_i$ changes in body-wall muscle cells expressing GCaMP2 were monitored by imaging GCaMP2 fluorescence intensity using an electron-multiplying CCD camera (iXon^{EM}+885, Andor Technology, Belfast, Northern Ireland), a FITC filter (59222, Chroma Technology Corp., Bellows Falls, VT, USA), a light source (Lambda XL, Sutter Instrument, Novato, CA, USA) and the NIS-Elements software (Nikon). TTL signals from the camera were used to synchronize the recordings of Ca^{2+} transients and the membrane potential in some experiments.

Data analyses

A train of spikes was defined as five or more spikes with an interval between two consecutive spikes of no more than 2 s. To avoid complications by overlapping events and baseline drift, 10 APs with a clear baseline before the AP and a clear AHP following the repolarization were randomly chosen from the recordings of each cell for quantifying spike amplitude, 10–90% rise time, 90–10% decay time, width and AHP amplitude. The resting membrane potential of each cell was measured from an interval when there were no spikes and no large postsynaptic potentials. All quantification was performed using the Clampfit software (version 10, Molecular Devices).

For Ca^{2+} imaging data, a single muscle cell of each preparation was chosen as region of interest (ROI). The fluorescence intensity in the ROI over successive frames was first plotted as absolute fluorescence intensity over time using the NIS-Elements software (Nikon, Tokyo, Japan), and then converted to F/F_0 using the MATLAB software (The MathWorks, Inc., Natick, MA, USA) running a custom module.

Data graphing and statistical analyses were performed with Origin (version 8, OriginLab, Northampton, MA, USA). Statistical comparisons were made either by unpaired *t* test or one-way ANOVA (followed by Bonferroni *post hoc* test) depending on whether the number of groups for comparison was two or more. All values are shown as mean ± S.E.M. $P < 0.05$ is considered to be statistically significant.

Results

Body-wall muscle APs are all-or-none events

Body-wall muscle APs were recorded in the classical whole-cell patch-clamp configuration, using extracellular and pipette solutions that are routinely used for recording postsynaptic currents at the *C. elegans* neuromuscular junction (Richmond & Jorgensen, 1999). In the absence of current injection, muscle cells fired all-or-none overshooting APs spontaneously, which generally occurred in trains (Fig. 1*A*). The firing of APs typically lasted for several minutes (mean ∼4 min) after the whole-cell configuration was achieved. Subsequently, APs stopped firing rather than becoming graded. The disappearance of APs was accompanied by a rundown of inward currents (Fig. 1*E*), which appeared to be caused by dialysis of intracellular factors rather than deterioration of the preparation, as other cells could still fire APs normally after

the first patch-clamped cell stopped firing. Therefore, we restricted our analyses to the period when AP firing could be observed.

A train of spikes was often preceded by a gradual elevation of the resting membrane potential (slow wave). Individual spikes within a train were usually followed by repolarization to near the resting membrane potential (Fig. 1*A* and *B*). We quantified spike peak amplitude, width (at 50% peak amplitude), 10–90% rise time, 90–10% decay time, and the amplitude of AHP, as were defined in Fig. 1*B*. In addition, we quantified the number of spikes per train as well as the duration of inter-spike intervals between consecutive events within a train (Fig. 1*C* and *D*). These analyses revealed several prominent features of body-wall muscle APs. First, all APs are overshooting all-or-none events that depolarize to approximately +20 mV. Second, the rate of rise of the AP is slower than the decay (repolarization). And third, the width of APs in *C. elegans* body-wall muscle (~20 ms) is much longer than that in vertebrate skeletal muscle (<2 ms) (Cooke & Grinnell, 1964; Redfern *et al.* 1970; Cruz *et al.* 1985; Wolters *et al.* 1994; Cairns *et al.* 2003).

Our observation of all-or-none APs contradicts a previous report that APs in *C. elegans* body-wall muscle cells are graded events (Jospin *et al.* 2002). To exclude the possibility that this discrepancy resulted from differences in recording solutions, we also recorded APs using the bath and pipette solutions reported in the previous study. All-or-none overshooting APs were also observed with these solutions (Supplementary Fig. S1). The resting membrane potential measured with the two sets of solutions were also similar (−26.9 ± 0.5 mV with standard solutions; −27.5 ± 0.6 mV with the solutions of Jospin *et al.* 2002), and consistent with our previous report

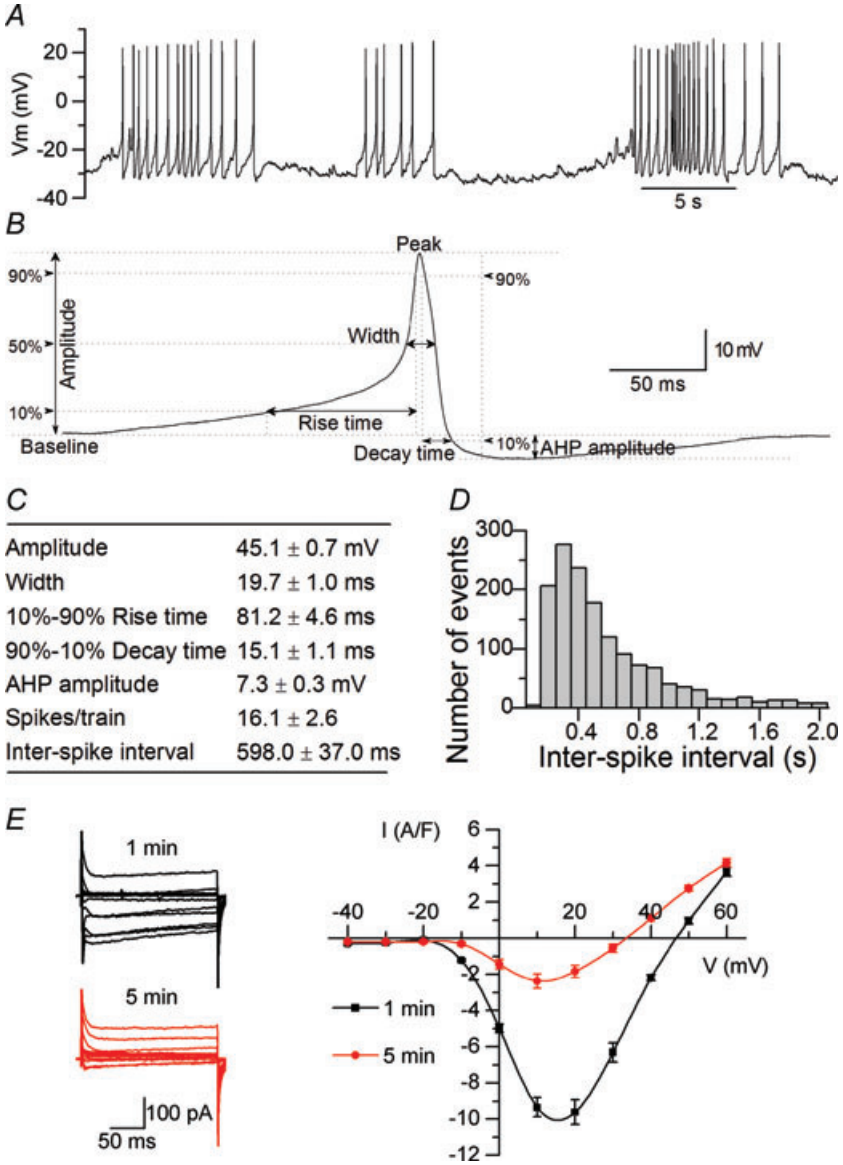

Figure 1. Action potentials (APs) in body-wall muscle cells of wild-type *C. elegans*
A, a representative trace of APs. *B*, a sample spike showing how the different parameters were measured. The difference between the pre-spike baseline and the post-spike undershoot (the most negative point) was defined as afterhyperpolarization (AHP). *C*, quantification of spike parameters. Spikes often occurred in trains. A train is defined as a minimum of 5 spikes with inter-spike intervals of <2 s. Values are shown as mean ± S.E.M. *D*, distribution of inter-spike intervals in spike trains. Shown are data of 25 recorded cells. *E*, inward currents showed time-dependent rundown after achieving the whole-cell patch clamp configuration. Shown are the representative traces and current–voltage relationship of inward currents at 1 and 5 min of 10 cells. Current amplitude was normalized by whole-cell membrane capacitance.

(−27.1 ± 0.8 mV) (Liu *et al.* 2006), but was substantially more negative than that reported by the previous study (−19.7 ± 1.8 mV) (Jospin *et al.* 2002).

The resting membrane potential in our study appeared to be near the threshold for AP firing because the slow waves that preceded APs were typically less than 10 mV above the resting membrane potential. To assess sensitivity of AP firing to the resting membrane potential, we analysed the effect of hyperpolarization (approximately −40 mV) on AP firing by injecting a small negative current. In all of the cells analysed ($n = 3$), the firing of APs stopped during the current injection and resumed after the current injection was terminated. A representative experiment is shown in Supplementary Fig. S2. Thus, rather than operating through graded potentials, *C. elegans* locomotory muscle cells generate all-or-none APs, and the rate of AP firing appeared to be very sensitive to membrane potential changes.

Body-wall muscle APs could occur after postsynaptic receptors were blocked

C. elegans body-wall muscle cells are innervated by cholinergic and GABAergic motoneurons (Chalfie & White, 1988; Wang, 2010). Cholinergic motoneurons release ACh to contract the muscle whereas GABAergic motoneurons release γ-aminobutyric acid (GABA) to relax the muscle. To determine whether AP firing requires neural input, we first analysed APs in the *unc-49(e407)* mutant, which lacks GABA receptors (Bamber *et al.* 1999), in the presence of the ACh receptor blocker d-tubocurarine (TBC). Under such experimental conditions, both cholinergic and GABAergic neuromuscular transmissions are blocked (Richmond & Jorgensen, 1999; Liu *et al.* 2005). Nevertheless, overshooting APs continued to occur with only altered resting membrane potential and spike amplitude (Fig. 2). These observations suggest that AP firing did not rely on neuromuscular transmission under the current experimental conditions.

Ca^{2+} channels underlie body-wall muscle APs

The lack of a candidate voltage-gated Na^+ channel in the *C. elegans* genome (Bargmann, 1998), and the fact that voltage-dependent inward currents in *C. elegans* body-wall muscle cells are abolished by the Ca^{2+} channel blocker Cd^{2+} (Jospin *et al.* 2002) suggest that Ca^{2+} serves as the charge carrier in the depolarizing phase of all-or-none APs. To assess the role of extracellular Ca^{2+}, we first tested the effect of adding Cd^{2+} (500 μM) to the standard extracellular solution, and found that this eliminated APs (Fig. 3*A*). We next tested the effects of different concentrations of extracellular Ca^{2+} on AP firing. All-or-none overshooting APs were always observed with 1 or 5 mM $[Ca^{2+}]_o$ but never with 200 or 500 μM $[Ca^{2+}]_o$, and the amplitude of APs was significantly lower at 1 mM than at 5 mM $[Ca^{2+}]_o$ (Fig. 3). These observations with different $[Ca^{2+}]_o$ confirmed the importance of Ca^{2+} entry in generating muscle APs. Interestingly, non-overshooting plateau potentials were sometimes observed at 500 μM $[Ca^{2+}]_o$ (not shown), suggesting that this $[Ca^{2+}]_o$ was near but not above the threshold for overshooting APs, and probably insufficient for triggering fast repolarization. Adding Cd^{2+} to the extracellular solution also resulted in a significantly less negative resting membrane potential (−13.2 ± 0.7 mV) (Fig. 3), which presumably resulted from decreased activity of Ca^{2+}-activated K^+ channel(s) (e.g. SLO-2) that are important to setting the resting membrane potential (see below). However, reducing $[Ca^{2+}]_o$ from 5 mM to 200 μM hyperpolarized the cells (Fig. 3*B*), although the mechanism underlying this effect is currently unclear.

We next determined which Ca^{2+} channel(s) carries the inward currents that underlie body-wall muscle APs. As null mutants of EGL-19, the predominant inward current carrier in *C. elegans* body-wall muscle cells (Jospin *et al.* 2002), are not viable (Lee *et al.* 1997) and nifedipine only blocks ∼50% of inward currents in *C. elegans* body-wall muscle cells (Jospin *et al.* 2002), we tested the effect of nemadipine-A, a putative specific blocker of the EGL-19 channel (Kwok *et al.* 2006). Application of nemadipine-A (3 μM) eliminated APs (Fig. 4*A*) as well as whole-cell inward currents (Supplementary Fig. S3) of body-wall muscle cells. To further confirm the importance of EGL-19, we analysed APs in *egl-19(ad695)*, a putative gain-of-function (*gf*) mutant (Lee *et al.* 1997). Both AP width and decay time were greatly increased in this mutant compared with wild-type (Fig. 4), consistent with EGL-19 channels carrying inward current during the AP. Surprisingly, the amplitudes of both APs and AHPs were significantly decreased in *egl-19(gf)* mutant worms (Fig. 4), suggesting that the mutated channel may have other unusual properties.

In addition to EGL-19, we investigated the role of CCA-1, UNC-2, NCA-1, and NCA-2 channels in spike generation by analysing APs in null mutants, including *cca-1(ad1650)*, *unc-2(e55)* and the double mutant *nca-1(gk9);nca-2(gk5)* (Shtonda & Avery, 2005; Bauer Huang *et al.* 2007; Jospin *et al.* 2007; Yeh *et al.* 2008). APs displayed normal depolarization and repolarization in the *nca-1;nca-2* strain (Fig. 4). By contrast, APs in the *unc-2* mutant showed increases in AHP amplitude and inter-spike interval relative to the wild-type (Fig. 4), while APs in the *cca-1* mutant displayed lower amplitude, longer decay time, wider peak and more spikes per train (Fig. 4). These observations suggest that the T-type Ca^{2+} channel CCA-1 also probably plays a role in generating and shaping muscle APs. However, the effect of *unc-2* mutation was probably indirect and resulted from deficient neuromuscular transmission because (1) UNC-2

expression in body-wall muscle cells was not detected (www.wormbase.org) and (2) neurotransmitter release at the *C. elegans* neuromuscular junction is greatly decreased in the *unc-2(e55)* mutant (Richmond *et al.* 2001).

K^+ channels shape muscle APs

Our previous study with cultured *C. elegans* embryonic body-wall muscle cells showed that outward currents are mainly carried by three K^+ channels, including the two voltage-gated channels SHL-1 and SHK-1, and the Ca^{2+}/Cl^--gated channel SLO-2 (Santi *et al.* 2003). SHL-1 carries fast transient, whereas SHK-1 and SLO-2 carry sustained, outward currents (Santi *et al.* 2003). The importance of SLO-2 in carrying sustained outward currents was also confirmed by recording whole-cell currents from body-wall muscle cells *in situ* (Santi *et al.* 2003; Yuan *et al.* 2003). To determine whether these K^+ channels are important in shaping muscle APs, we analysed APs in *shl-1(ok1168)*, *shk-1(ok1581)* and *slo-2(nf101)*. *shl-1(ok1168)* and *slo-2(nf101)* are putative nulls resulting from deletions (Yuan *et al.* 2003; Fawcett *et al.* 2006). *shk-1(ok1581)* was also a deletion mutant but the precise region of deletion was unclear. We sequenced the genomic DNA of this mutant and found a 634 bp deletion (9766598–9767231 on chromosome II) plus an 8 bp insertion (CTAAATAT), which resulted in a mutation of methionine 252 to isoleucine (based on amino acid number of the ZK1321.2c isoform, www.wormbase.org) followed by a stop codon. This mutation eliminates essentially all amino acid residues following the T1 domain (Wei *et al.* 1996).

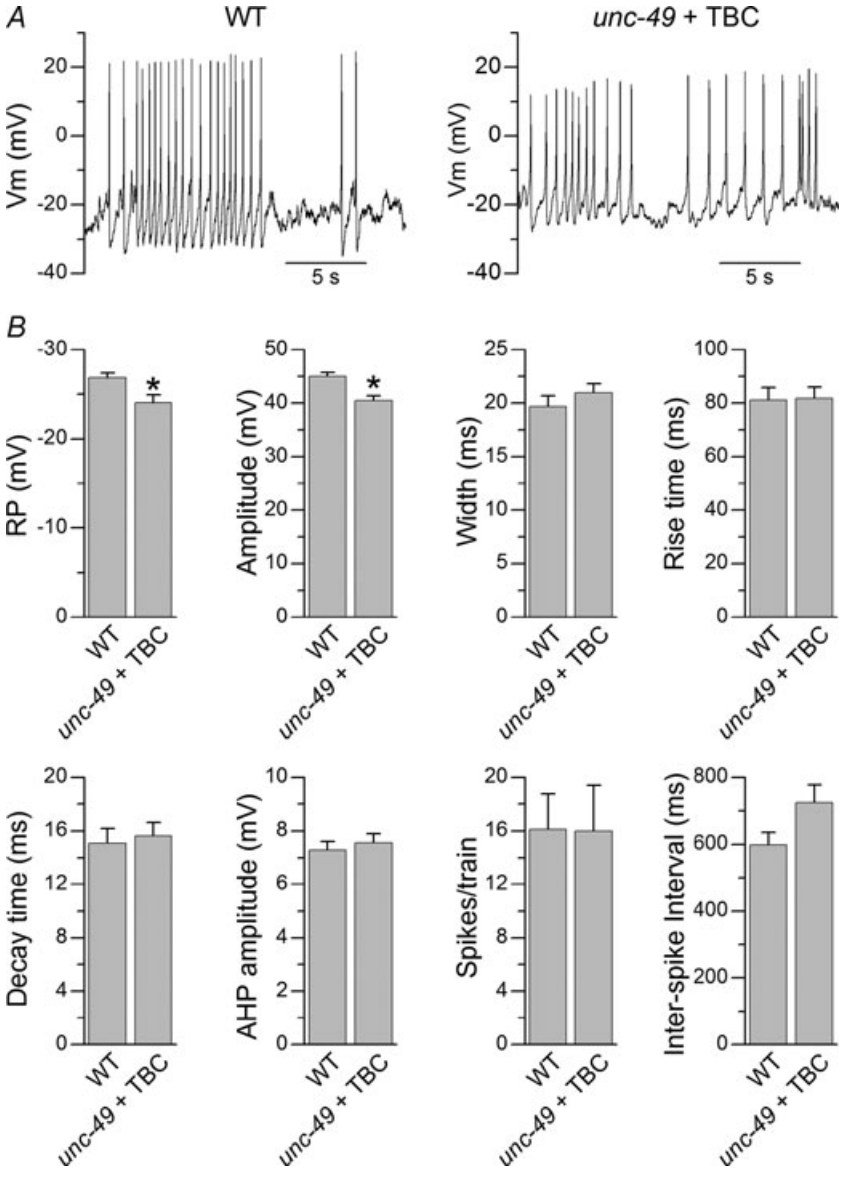

Figure 2. *C. elegans* body-wall muscle cells did not require neural input to fire action potentials (APs)
Both cholinergic and GABAergic neural inputs to muscle cells were blocked by administering the acetylcholine receptor blocker d-tubocurarine (TBC) to the *unc-49(e407)* mutant, which lacks GABA receptors. *A*, sample AP traces from muscle cells of the wild-type (WT) and the *unc-49* mutant treated with TBC (*unc-49* + TBC). *B*, comparisons of the resting membrane potential (RP), spike properties and afterhyperpolarization (AHP) amplitude between WT and *unc-49* + TBC. Values are shown as mean ± S.E.M. The asterisk indicates a statistically significant difference compared with WT ($P < 0.05$, unpaired *t* test). The number of cells analysed was 25 for the WT and 26 for *unc-49* + TBC.

shl-1(ok1168) did not show any significant change in AP parameters when compared with the wild-type (Fig. 5). In contrast, APs from *shk-1(ok1581)* showed increases in spike amplitude, width, decay time and AHP amplitude, and a decrease in the number of spikes per train (Fig. 5). The increase in spike amplitude suggests that SHK-1 is activated during the AP upstroke and plays an important role in initiating repolarization while the increase in spike width suggests that SHK-1 is important to repolarization. The larger AHP amplitude was presumably because of enhanced activation of Ca^{2+}-activated K^+ channels as a result of increased Ca^{2+} entry associated with spike broadening. The decrease in the number of spikes per train could be secondary to the increase in AHP amplitude.

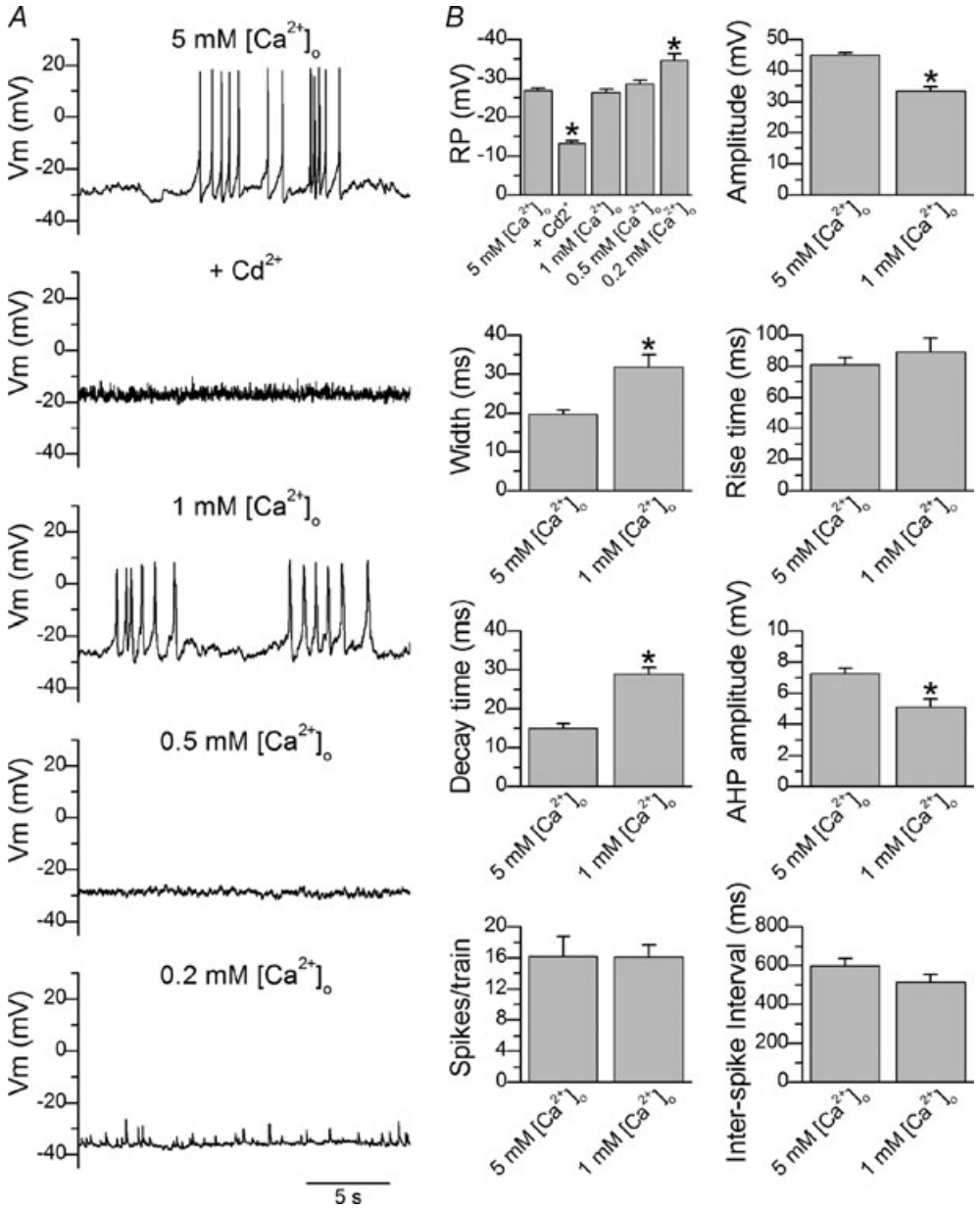

Figure 3. Extracellular Ca^{2+} was essential to the occurrence of action potentials in *C. elegans* body-wall muscle cells

A, sample action potential (AP) traces from body-wall muscle cells of wild-type worms in the presence of the standard extracellular solution (5 mM $[Ca^{2+}]_o$), standard extracellular solution with 0.5 mM Cd^{2+} (+ Cd^{2+}) and solutions with reduced $[Ca^{2+}]_o$ (1 mM, 0.5 mM or 0.2 mM). Overshooting APs were always observed at 1 or 5 mM $[Ca^{2+}]_o$ but never at 0.2 or 0.5 mM $[Ca^{2+}]_o$ or in the presence of Cd^{2+}. *B*, comparisons of the resting membrane potential (RP), spike properties and afterhyperpolarization (AHP) amplitude. The asterisk indicates a statistically significant difference compared with 5 mM $[Ca^{2+}]_o$ ($P < 0.05$, unpaired *t* test or ANOVA with Bonferroni *post hoc* test). All values are shown as mean ± S.E.M. The number of cells analysed was 25 for 5 mM $[Ca^{2+}]_o$, 11 for + Cd^{2+}, 9 for 1 mM $[Ca^{2+}]_o$, 10 for 0.5 mM $[Ca^{2+}]_o$ and 9 for 0.2 mM $[Ca^{2+}]_o$.

Thus, SHK-1 plays important roles in repolarization and in regulating the pattern of AP firing.

Like the *shk-1* mutant, *slo-2(nf101)* showed an increase in both AP width and decay time compared with the wild-type. In addition, the *slo-2* mutant exhibited a lower (less negative) resting membrane potential, a smaller AHP amplitude, a shorter inter-spike interval, and the occurrence of long-duration (>2 s) all-or-none membrane depolarizations, which may be referred to as plateau potentials (Lockery & Goodman, 2009) (Fig. 6). The plateau potentials frequently appeared as the last one or two events in a train of APs but sometimes

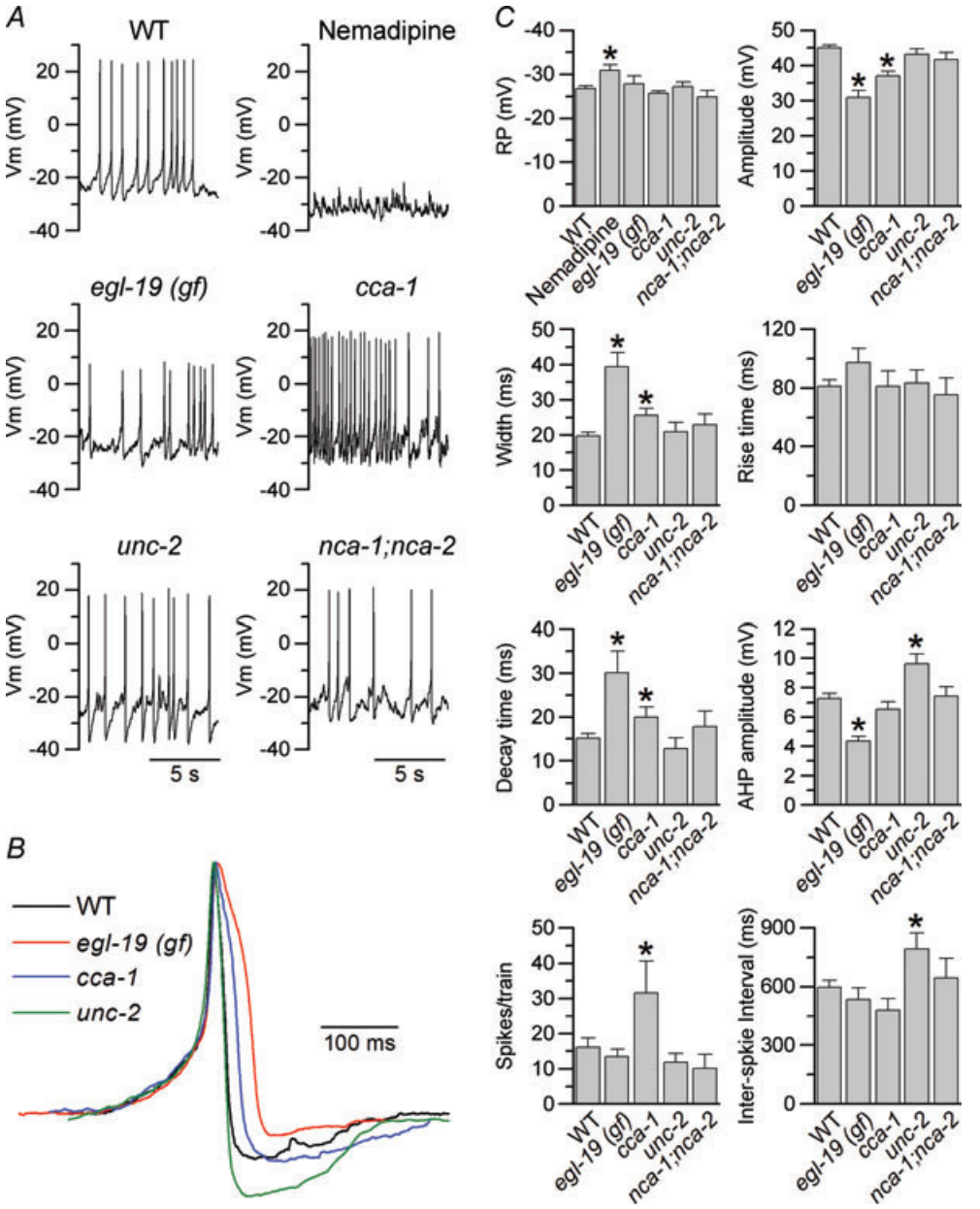

Figure 4. The L-type Ca^{2+} channel EGL-19 was essential while the T-type Ca^{2+} channel CCA-1 was also implicated in generating action potentials (APs) in *C. elegans* body-wall muscle
A, sample AP traces from the wild-type (WT), WT treated with 3 μM nemadipine-A, *egl-19(ad695)*, *cca-1(ad1650)*, *unc-2(e55)* and the double mutant *nca-1(gk9):nca-2(gk5)*. *egl-19(ad695)* is a putative gain-of-function mutant whereas the others are loss-of-function mutants. *B*, representative APs of selected groups are shown superimposed. *C*, comparisons of the resting membrane potential (RP), spike properties and afterhyperpolarization (AHP) amplitude between WT and the other groups. The asterisk indicates a statistically significant difference compared with WT ($P < 0.05$, one-way ANOVA with Bonferroni *post hoc* tests). The number of cells analysed was 25 for WT, 10 for nemadipine, 6 for *egl-19(gf)*, 11 for *cca-1(lf)*, 11 for *unc-2(lf)* and 6 for *nca-1(lf):nca-2(lf)*.

occurred repeatedly (Fig. 6*A*). These observations suggest that SLO-2 regulates body-wall muscle excitability in several ways, including setting the resting membrane potential, facilitating spike repolarization, enhancing AHP and prolonging the inter-spike interval.

To assess the combined effects of SHK-1 and SLO-2, we built *shk-1(ok1581);slo-2(nf101)* double mutant worms and analysed APs in this strain. While the *slo-2* mutant showed plateau potentials as well as typical APs, the double mutant showed exclusively plateau potentials (Fig. 6). The duration of plateau potentials was significantly longer in the double mutant (4.4 ± 0.4 s) than in *slo-2* single mutant (2.8 ± 0.3 s) ($P < 0.05$, unpaired *t* test). A significant increase in AP amplitude was observed in the double mutant compared with wild-type (54 ± 2.2 mV *versus* 45.1 ± 0.7 mV) (Fig. 6*A*), which was also seen in the single

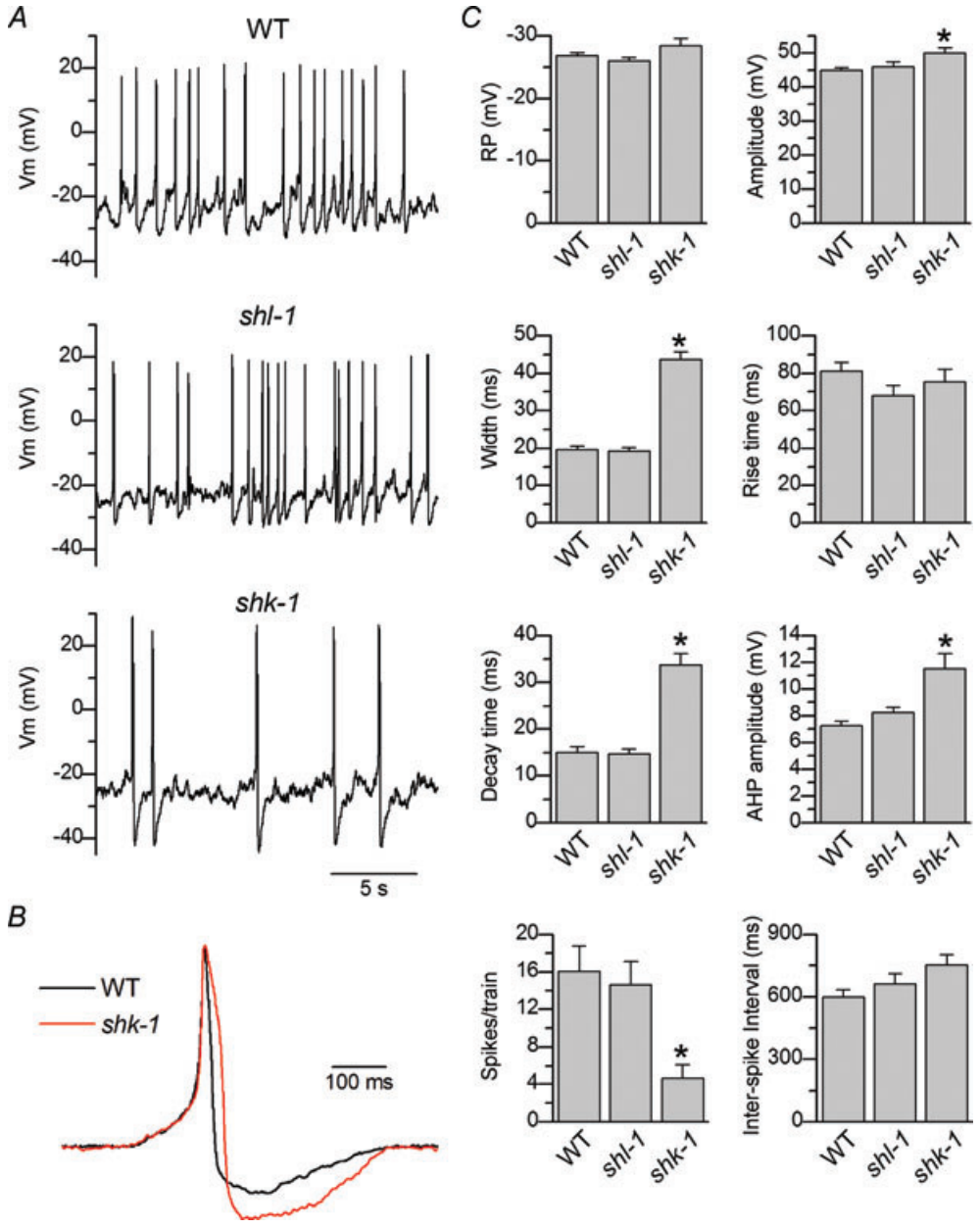

Figure 5. The *Shaker* K$^+$ channel SHK-1 but not the *Shal* K$^+$ channel SHL-1 regulated action potential (AP) waveform and firing pattern in *C. elegans* body-wall muscle cells
A, sample AP traces from the wild-type (WT), and the loss-of-function (*lf*) mutants *shl-1(ok1168)* and *shk-1(ok1581)*. *B*, representative APs of the WT and *shk-1* mutant are shown superimposed. *C*, comparisons of the resting membrane potential (RP), spike properties and afterhyperpolarization (AHP) amplitude between WT and the other groups. The asterisk indicates a statistically significant difference ($P < 0.05$, one-way ANOVA with Bonferroni *post hoc* tests). The number of cells analysed was 25 for WT, 8 for *shl-1(lf)* and 8 for *shk-1(lf)*.

mutant of *shk-1* but not *slo-2*. Thus, the changes observed in the double mutant were consistent with the combined effects of the two single mutants.

The effects of *shk-1* and *shk-1:slo-2* mutations on whole-cell currents had not been analysed in body-wall muscle cells *in situ*, which could differ from the previously analysed cultured embryonic muscle cells in ion channel function and expression. To substantiate the roles of SHK-1 and SLO-2 in shaping APs, we compared the amplitude of whole-cell outward currents among the wild-type, *shk-1(ok1581)*, *slo-2(nf101)* and the double mutant *shk-1(ok1581):slo-2(nf101)*. Sustained outward currents were significantly decreased in either single mutant, and essentially absent in the double mutant (Fig. 7). Thus, SHK-1 and SLO-2 play key roles in shaping muscle APs by acting as major outward current carriers.

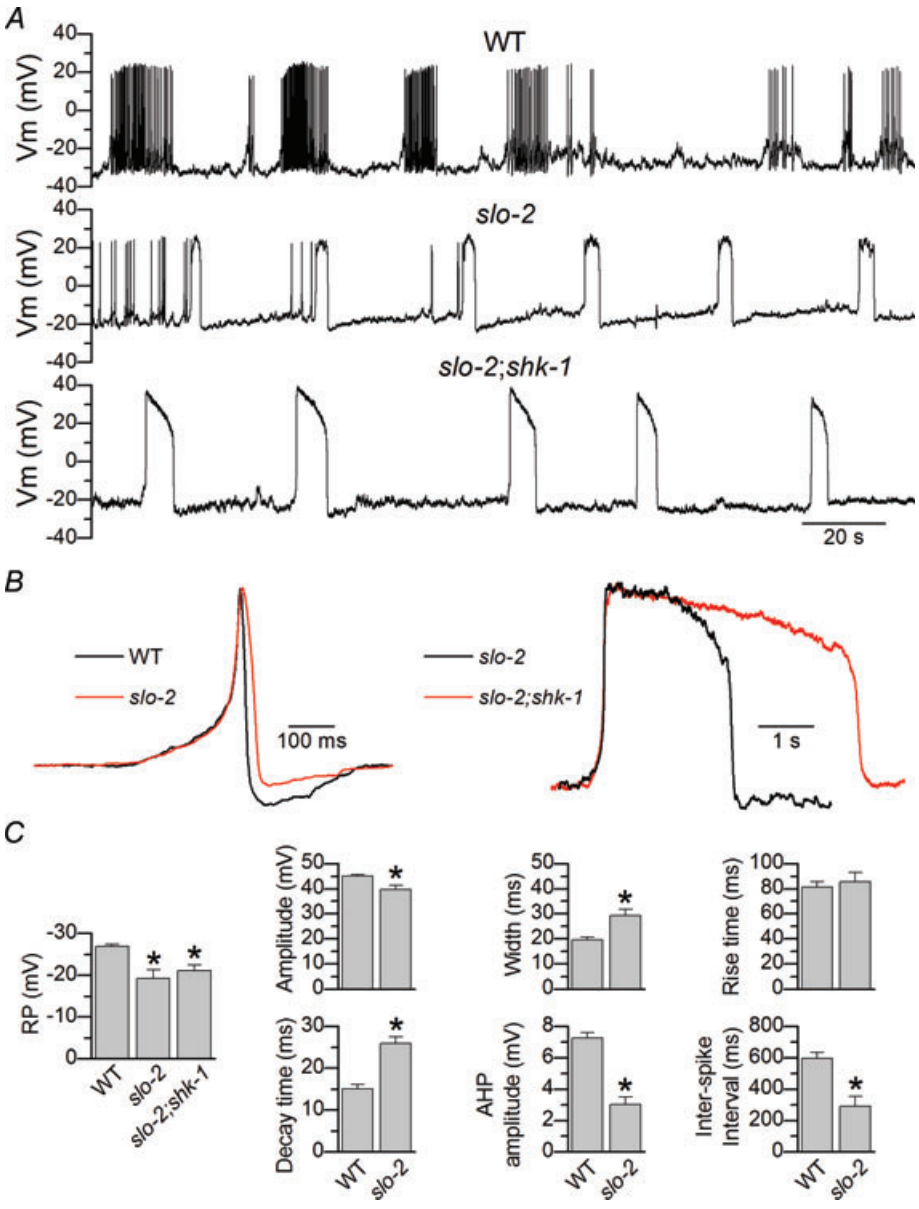

Figure 6. The Ca^{2+}- and Cl^{-}-gated K^{+} channel SLO-2 was important to setting the resting membrane potential and shaping the action potential (AP) waveform in *C. elegans* body-wall muscle cells
A, sample AP traces from the wild-type (WT), *slo-2(nf101)* and the *slo-2(nf101):shk-1(ok1581)* double mutant. *B*, representative APs from the WT and *slo-2* mutant (left), and plateau potentials from *slo-2* single mutant and *slo-2:shk-1* double mutant (right) shown superimposed. The double mutant showed only plateau potentials. *C*, comparisons of the resting membrane potential (RP), spike properties and afterhyperpolarization (AHP) amplitude between WT and the other groups. The asterisk indicates a statistically significant difference ($P < 0.05$, unpaired *t* test or one-way ANOVA with Bonferroni *post hoc* tests). Plateau potentials of the *slo-2* mutant were excluded in these comparisons. The number of cells analysed was 25 for WT, 9 for *slo-2* and for 8 *slo-2:shk-1*.

AP firing is associated with an elevation of intracellular [Ca^{2+}] and muscle contraction

Elevation of $[Ca^{2+}]_i$ is a key step initiating contraction in all myocytes. To determine how AP firing is related to Ca^{2+} mobilization and contraction, we analysed the temporal correlation between spike firing and $[Ca^{2+}]_i$ in worms expressing the genetically encoded Ca^{2+} indicator GCaMP2 (Tallini *et al.* 2006) in body-wall muscle cells under the control of P*myo-3* (Okkema *et al.* 1993). To improve expression *in vivo*, GCaMP2 was synthesized for *C. elegans* codon optimization and insertion of two introns. APs and Ca^{2+} transients were recorded simultaneously *in vivo* in dissected worms. APs recorded from muscle cells expressing GCaMP2 were variable in amplitude (Fig. 8*A*), probably a consequence of increased Ca^{2+} buffering by the intrinsic calmodulin domain of GCaMP2 (Tallini *et al.* 2006). Nevertheless, a correlation between AP firing and Ca^{2+} transients was observed, with a single Ca^{2+} transient peak often associated with a train of spikes, and smaller Ca^{2+} transients associated with fewer spikes (Fig. 8). Moreover, imaging experiments demonstrated that the elevations of $[Ca^{2+}]_i$ were associated with muscle twitches (Supplementary Movie 1). A temporal correlation between Ca^{2+} transients and muscle contractions was established by measurements of the length of selected muscle cells in preparations in which Ca^{2+} transients had been measured (Fig. 9). Finally, we confirmed that Ca^{2+} transients could occur in the absence of neuromuscular transmission by recording Ca^{2+} transients in *unc-49(e407)* mutant worms in the presence of 0.5 mM d-TBC (Supplementary Fig. S4 and Supplementary Movie 2), which is in agreement with our observations of APs (Fig. 2).

The observations that APs and Ca^{2+} transients continued to occur in the absence of neuromuscular transmission were made with dissected worms in the presence of artificial extracellular and intracellular solutions, which raised the question as to whether body-wall muscle cells can indeed generate APs and Ca^{2+} transients spontaneously under physiological conditions. To answer this question, we recorded Ca^{2+} transients in intact worms of the wild-type as well as mutants that are deficient either in postsynaptic receptors or presynaptic release ability. Ca^{2+} transients were observed in all the strains that we analysed, including the wild-type, *unc-49(e407)*, which lacks $GABA_A$ receptors (Bamber *et al.* 1999), *unc-63(x37):acr-16(ok789)*, which lacks all acetylcholine receptors in body-wall muscle cells (Culetto *et al.* 2004; Francis *et al.* 2005; Touroutine *et al.* 2005) and *unc-64(e246)*, which is severely defective in releasing neurotransmitters due to a mutation in the syntaxin gene (Wang *et al.* 2001) (Supplementary Fig. S5 and Supplementary Movies 3–6). These findings support the notion that body-wall muscle cells have intrinsic abilities to fire APs, since Ca^{2+} transients are associated with AP firing.

Both EGL-19 and UNC-68 are required for Ca^{2+} transients in muscle cells

Finally, we analysed the roles of EGL-19 and UNC-68 in the Ca^{2+} transients triggered by APs in body-wall muscle cells. These cytosolic Ca^{2+} transients could result from Ca^{2+} entry through VGCCs in the plasma membrane, Ca^{2+} release through RyRs in the SR membrane, or both. To determine whether EGL-19 and UNC-68 are required for the elevation of $[Ca^{2+}]_i$, we tested the effect of nemadipine-A on Ca^{2+} transients in wild-type worms, and analysed Ca^{2+} transients in *unc-68(r1162)*, which is a null mutant of the single RyR gene in *C. elegans* (Maryon *et al.* 1996). We found that muscle Ca^{2+} transients

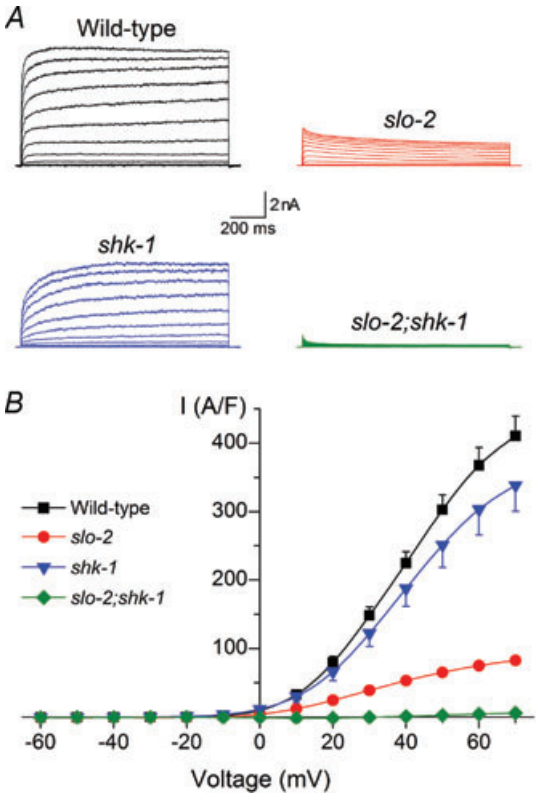

Figure 7. SLO-2 and SHK-1 K^+ channels were primary carriers of sustained outward currents in body-wall muscle cells
A, Sample traces of whole-cell currents from wild-type, *slo-2(nf101)*, *shk-1(ok1581)*, and the double mutant *slo-2(nf101); shk-1(ok1581)* in response to voltage steps of −60 to +70 mV (1200 ms duration) at 10-mV intervals from a holding potential of −60 mV. *B*, Current (I)–voltage relationships of the different groups. Each data point (mean ± S.E.M.) represents the mean current amplitude during the last 200 ms of the voltage step. The current–voltage relationship was significantly different between the different groups (Kolmogorov–Smirnov test). The number of cells analysed was 11 for wild-type, and 9 for each of the remaining groups.

were abolished in wild-type worms by nemadipine-A and never observed in *unc-68* mutant worms (Fig. 10, Supplementary Movies 7 and 8). Thus, both the sarcolemmal Ca^{2+} channel EGL-19 and the sarcoplasmic reticulum RyR channel UNC-68 are necessary to produce muscle Ca^{2+} transients, which is similar to mammalian cardiac and striated muscles.

Discussion

Regenerative membrane potential changes may be classified as APs, graded potentials, plateau potentials and intrinsic oscillations (Lockery & Goodman, 2009). APs are all-or-none events with a stereotypical waveform; graded potentials change amplitude and waveform according to the strength and waveform of the stimulus; plateau potentials are prolonged all-or-none depolarizations; and intrinsic oscillations are slow, cyclic alternations in the membrane potential (Lockery & Goodman, 2009). Our data indicate that *C. elegans* body-wall muscle cells generate all-or-none APs with a stereotypical waveform.

Several lines of evidence suggest that Ca^{2+} entry through the L-type Ca^{2+} channel EGL-19 plays a key role in generating muscle APs. First, APs were eliminated when the standard extracellular solution was modified by either reducing $[Ca^{2+}]$ or adding the Ca^{2+} channel blocker Cd^{2+}. Second, blocking EGL-19 with nemadipine-A abolished APs whereas a gain-of-function mutation of *egl-19* increased spike width and decay time. Third, overshooting spikes continued to occur under experimental conditions when Na^+ flow could not possibly be responsible for them (details in the next paragraph). Besides EGL-19, CCA-1 might also play a role in generating or shaping muscle spikes, as the *cca-1* mutant showed several significant changes in spike properties, including decreased spike amplitude, and increased spike width, decay time, and number of spikes per train. However, except for the decreased spike amplitude, the other changes are more easily interpreted as resulting from developmental changes caused by *cca-1(lf)*, such as a compensatory increase in EGL-19 expression. Although further studies are needed to completely understand the roles of these two Ca^{2+}

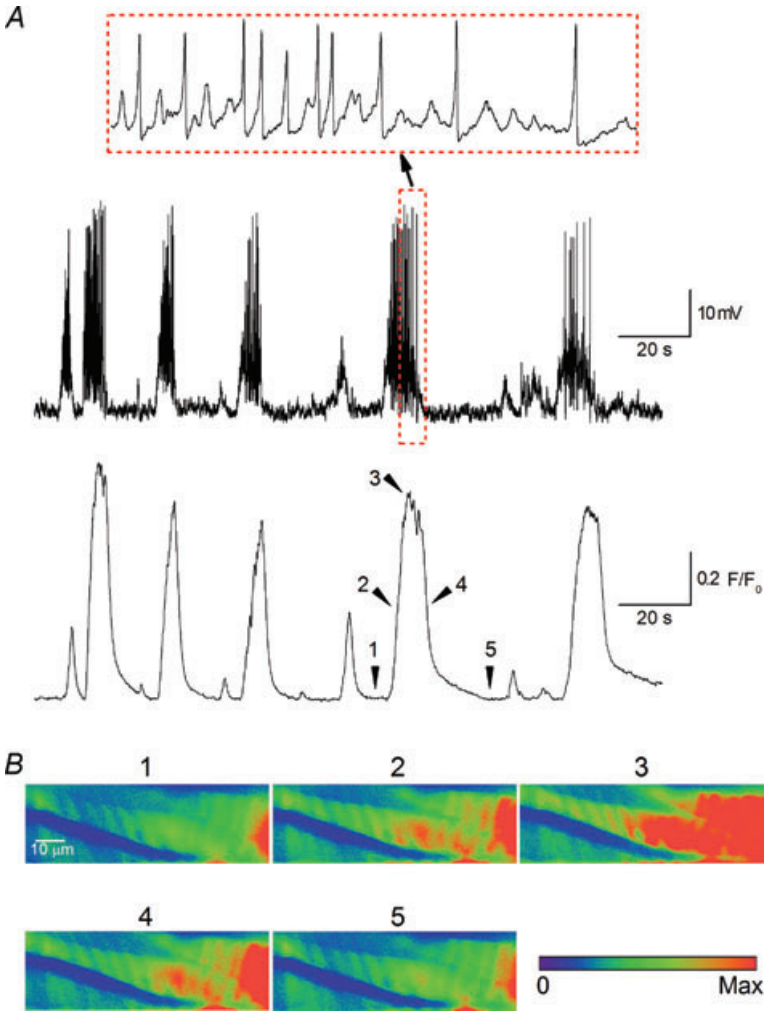

Figure 8. Action potential (AP) trains were associated with increases of intracellular $[Ca^{2+}]$ in *C. elegans* body-wall muscle cells
A, simultaneous recordings of muscle APs and Ca^{2+} transients showing a temporal correlation between Ca^{2+} transients and AP firing. A portion of the membrane potential trace was expanded and is shown at a shorter time scale, as indicated by the red rectangular box. *B*, Ca^{2+} imaging from the selected time points indicated in *A*. Ca^{2+} transients were detected by imaging the fluorescence of GCaMP2 expressed in body-wall muscle cells. Shown is a representative of 10 similar experiments.

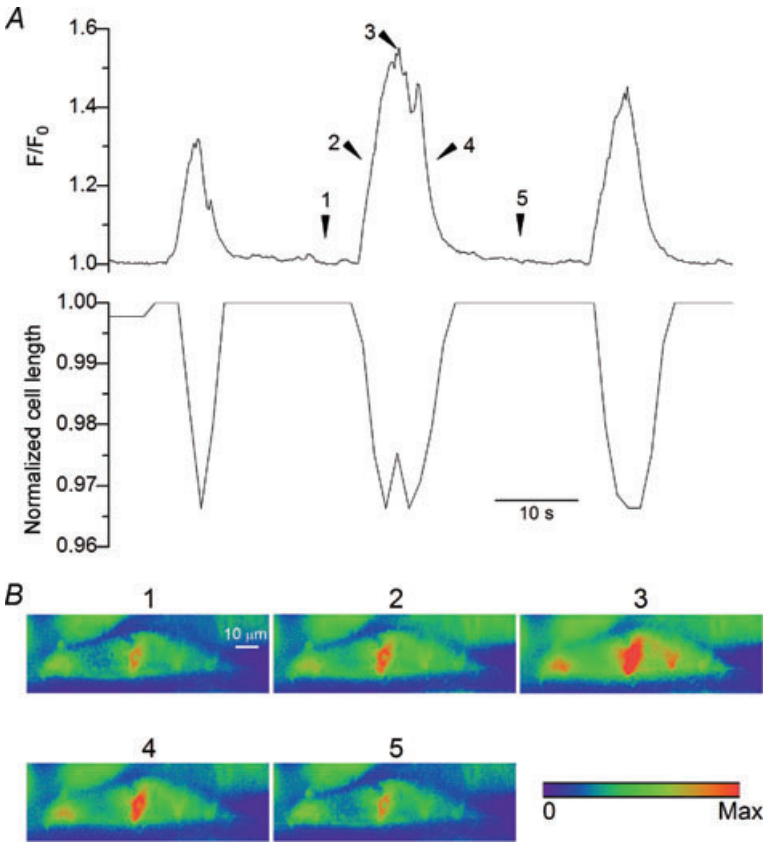

Figure 9. Elevations of intracellular [Ca^{2+}] were associated with shortening of *C. elegans* body-wall muscle cells
A, Ca^{2+} transients of a selected body-wall muscle cell. *B*, length over time plot for the selected body-wall muscle cell. Shown is a representative of 27 similar experiments. A movie of this experiment may be found in the Supplementary Movie 1.

channels in body-wall muscle APs, our observations with both mutants are consistent with the previous reports of *egl-19* and *cca-1* expression in *C. elegans* body-wall muscle cells (Lee *et al.* 1997; Steger *et al.* 2005), and of EGL-19 being a predominant carrier of inward current in these cells (Jospin *et al.* 2002).

While Ca^{2+} entry played a key role in generating APs, extracellular Na^+ was also implicated. Specifically, when $[Na^+]_o$ was reduced from 140 mM to 4 mM, all-or-none overshooting APs became rare events and had smaller amplitudes (Supplementary Fig. S6*A* and *B*). The all-or-none overshooting APs observed under

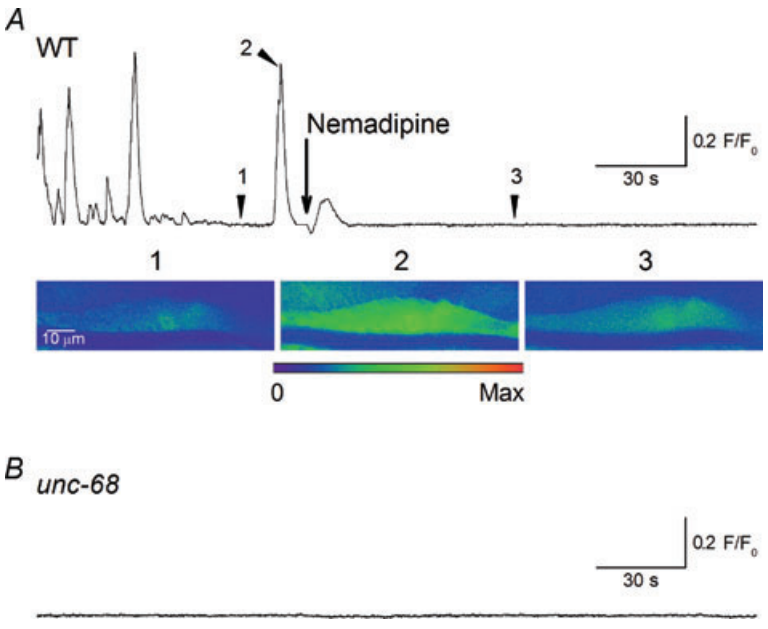

Figure 10. The occurrence of Ca^{2+} transients in *C. elegans* body-wall muscle cells required the functions of both the L-type Ca^{2+} channel EGL-19 and the ryanodine receptor UNC-68
A, application of the Ca^{2+} channel blocker nemadipine-A (10 μM) abolished Ca^{2+} transients in wild-type (WT) worms. The top panel shows Ca^{2+} transients of a representative experiment with the time point of adding nemadipine-A indicated by an arrow whereas the bottom panel shows Ca^{2+} imaging at the specified time points in the sample trace (indicated by arrowheads). *B*, Ca^{2+} transients were not detected in the null mutant *unc-68(r1162)*. *A* and *B* are representative of 12 and 7 similar experiments, respectively. Movies of the experiments shown in *A* and *B* may be found in the Supplementary Movies 7 and 8.

such experimental conditions were unlikely to be caused by Na^+ influx because the Na^+ equilibrium potential was −17.5 mV. The reduction of $[Na^+]_o$ also caused a decrease in whole-cell inward currents without altering the current–voltage relationship, which was characteristic of high voltage-gated Ca^{2+} channels (Supplementary Fig. S6*C*). There are at least two potential mechanisms for the observed effects of low $[Na^+]_o$: (1) a permissive level of extracellular Na^+ may be needed to effectively open VGCCs (e.g. EGL-19), and (2) EGL-19 and/or CCA-1 are not strictly selective for Ca^{2+}. While mammalian VGCCs are highly selective for Ca^{2+} over Na^+ (ratio >1000:1) (Tsien *et al.* 1987), it is unknown whether *C. elegans* VGCCs have a similarly high selectivity for Ca^{2+}. Therefore, how extracellular Na^+ contributes to AP firing and inward currents remains to be determined.

Loss-of-function mutation of either *shk-1* or *slo-2* delayed spike repolarization. In addition, SHK-1 dysfunction decreased the number of spikes per train while SLO-2 dysfunction caused lower (less negative) resting membrane potential, smaller AHP amplitude and shorter inter-spike interval. These observations suggest that SHK-1 facilitates repolarization and regulates AP firing pattern, and that SLO-2 plays several roles, including setting the resting membrane potential, facilitating AP repolarization, enhancing AHP and regulating the firing pattern. Facilitation of spike repolarization by SHK-1 appears to be a conserved function because spike broadening is also observed in mutants of the *Drosophila Shaker* K^+ channel (Tanouye *et al.* 1981; Salkoff, 1985). In contrast, all the functions uncovered for SLO-2 were previously unknown for itself as well as its homologues in other species. Given that SLO-2 and its mammalian homologues (Slo2.1/Slick and Slo2.2/Slack) are widely expressed in neurons and muscle cells (Yuan *et al.* 2000; Bhattacharjee *et al.* 2002; Dryer, 2003; Santi *et al.* 2003; Bhattacharjee *et al.* 2005; Budelli *et al.* 2009), and that their activities may be modulated by a variety of factors, including intracellular Cl^-, Ca^{2+}, Na^+ and pH (Yuan *et al.* 2000, 2003; Ruffin *et al.* 2008), neurotransmitters (Santi *et al.* 2006; Berg *et al.* 2007), nicotinamide adenine dinucleotide (NAD^+) (Tamsett *et al.* 2009), oestradiol (Zhang *et al.* 2005), Fragile X mental retardation protein (Brown *et al.* 2010) and hypoxia/ischaemia (Mitani & Shattock, 1992; Yuan *et al.* 2003), the regulation of the resting membrane potential, spike waveform and firing pattern by SLO-2/Slo2 could have far reaching implications in cellular activities. It would be interesting to investigate whether SLO-2/Slo2 also plays an important role in shaping spike waveform or regulating spike firing pattern in mammals or in other cells of *C. elegans*.

Our observations suggest that AP-induced elevation of $[Ca^{2+}]_i$ requires both *egl-19* and *unc-68* gene products; however, the relative contributions of extracellular Ca^{2+} entry and intracellular Ca^{2+} release, and the molecular linkage between these channels, remain to be established. The requirement for EGL-19 does not establish the importance of Ca^{2+} entry through it, since the major source of Ca^{2+} for muscle contractions could be the sarcoplasmic reticulum (SR), and the primary function of EGL-19 could be to activate the SR Ca^{2+}-release channel UNC-68 through either Ca^{2+}-induced Ca^{2+} release (Cannell *et al.* 1995; Verkhratsky & Shmigol, 1996; Kotlikoff, 2003) or direct protein–protein interactions between the L-type Ca^{2+} channel and ryanodine receptor (Schneider, 1994). Further investigations are needed to determine the role of Ca^{2+} entry and how UNC-68 may be activated in *C. elegans* body-wall muscle cells.

C. elegans body-wall muscle is controlled by cholinergic and GABAergic motoneurons, which contract and relax the muscle, respectively. The fact that spike trains continued to occur in the absence of neuromuscular transmission suggests that AP firing is probably an intrinsic property of body-wall muscle cells. Despite this intrinsic activity, motoneurons must play an important role in body-wall muscle AP firing under physiological conditions, through the modulation of muscle resting potential and the attendant effect on the AP firing pattern. This modulatory role of motoneurons is supported by pharmacological and genetic experiments. Neuromuscular blockade resulted in a decrease in the resting membrane potential and AP amplitude, suggesting tonic inhibitory control through GABAergic motoneurons. Moreover, mutations of UNC-2, the major Ca^{2+} channel controlling neurotransmitter release at the *C. elegans* neuromuscular junction (Richmond *et al.* 2001), resulted in an increase in inter-spike interval and AHP amplitude. While the mechanisms that underlie generation of the sinusoidal locomotory waveform are not well understood, the prevailing model enlists command interneurons and motoneurons as key players but body-wall muscle cells as simple actuators (de Bono & Maricq, 2005; Boyle & Cohen, 2008). This model does not explain the continued locomotory activities of mutant worms lacking both the levamisole-sensitive and nicotine-sensitive ACh receptors in body-wall muscle (Francis *et al.* 2005; Touroutine *et al.* 2005), however. Alternatively, the 'neurocratic' model proposes that propagation of electrical activity in muscle is the basis of locomotory waveform, and that the function of neurons is to modulate muscle activity (Crofton, 1971; Johnson & Stretton, 1980; Niebur & Erdos, 1988). In spite of the differences, these two models are not mutually exclusive and are consistent with a primary neuromodulatory role of *C. elegans* motoneurons.

The body-wall muscle APs reported here are distinct from those in *C. elegans* RMD interneurons and pharyngeal muscle cells. APs in RMD ring motor interneurons appear as membrane potential fluctuations between two stable levels (−70 and −20 mV) (Mellem *et al.* 2008), whereas those in pharyngeal muscle cells

have a long duration (mean > 200 ms) with a plateau phase (Franks *et al.* 2002) that resembles APs generated by mammalian cardiac myocytes. The depolarization phase of APs in *C. elegans* pharynx also relies on EGL-19 and CCA-1 channels (Shtonda & Avery, 2005), which is consistent with the lack of Na^+ channels in *C. elegans*, whereas the repolarization phase depends on the function of EXP-2, a voltage-gated K^+ channel (Davis *et al.* 1999; Shtonda & Avery, 2005).

C. elegans body-wall muscle has been considered to be analogous to mammalian skeletal muscle (Moerman & Fire, 1997; Lecroisey *et al.* 2007). However, results of the present study suggest that APs in *C. elegans* body-wall muscle cells differ from mammalian skeletal muscle at least in three major ways. First, APs are myogenic in *C. elegans* body-wall muscle, but neurogenic in mammalian skeletal muscle; second, the time course of APs in *C. elegans* body-wall muscle is much longer than that in mammalian skeletal muscle; and third, APs in *C. elegans* body-wall muscle result from the activation of VGCCs rather than voltage-gated Na^+ channels. The identities of ion channels important for spike repolarization also appear to be different between *C. elegans* body-wall muscle (K^+ channels) and mammalian skeletal muscle (Cl^- channels) (Hudson *et al.* 1995). Nevertheless, the finding that *C. elegans* body-wall muscle generates all-or-none APs brings the physiology of *C. elegans* muscle much closer to that of other metazoans, and strengthens its utility as a model organism.

References

Bamber BA, Beg AA, Twyman RE & Jorgensen EM (1999). The *Caenorhabditis elegans unc-49* locus encodes multiple subunits of a heteromultimeric GABA receptor. *J Neurosci* **19**, 5348–5359.

Bargmann CI (1998). Neurobiology of the *Caenorhabditis elegans* genome. *Science* **282**, 2028–2033.

Bauer Huang SL, Saheki Y, VanHoven MK, Torayama I, Ishihara T, Katsura I *et al.* (2007). Left-right olfactory asymmetry results from antagonistic functions of voltage-activated calcium channels and the Raw repeat protein OLRN-1 in *C. elegans*. *Neural Dev* **2**, 24.

Berg AP, Sen N & Bayliss DA (2007). TrpC3/C7 and Slo2.1 are molecular targets for metabotropic glutamate receptor signaling in rat striatal cholinergic interneurons. *J Neurosci* **27**, 8845–8856.

Bhattacharjee A, Gan L & Kaczmarek LK (2002). Localization of the Slack potassium channel in the rat central nervous system. *J Comp Neurol* **454**, 241–254.

Bhattacharjee A, von Hehn CA, Mei X & Kaczmarek LK (2005). Localization of the Na^+-activated K^+ channel Slick in the rat central nervous system. *J Comp Neurol* **484**, 80–92.

Boyle JH & Cohen N. (2008). Caenorhabditis elegans body wall muscles are simple actuators. *Biosystems* **94**, 170–181.

Brown MR, Kronengold J, Gazula VR, Chen Y, Strumbos JG, Sigworth FJ *et al.* (2010). Fragile X mental retardation protein controls gating of the sodium-activated potassium channel Slack. *Nat Neurosci.* **13**, 819–821.

Budelli G, Hage TA, Wei A, Rojas P, Jong YJ, O'Malley K & Salkoff L (2009). Na^+-activated K^+ channels express a large delayed outward current in neurons during normal physiology. *Nat Neurosci* **12**, 745–750.

Cairns SP, Buller SJ, Loiselle DS & Renaud JM (2003). Changes of action potentials and force at lowered $[Na^+]_o$ in mouse skeletal muscle: implications for fatigue. *Am J Physiol Cell Physiol* **285**, C1131–C1141.

Cannell MB, Cheng H & Lederer WJ (1995). The control of calcium release in heart muscle. *Science* **268**, 1045–1049.

Catterall WA (1986). Molecular properties of voltage-sensitive sodium channels. *Annu Rev Biochem* **55**, 953–985.

Chalfie M & White J (1988). The nervous system. In *The Nematode Caenorhabditis elegans*, The community of *C. elegans* researchers, ed. Wood WB, pp. 337–391. Cold Spring Harbor Laboratory Press, Plainview.

Cooke IM & Grinnell AD (1964). Effect of tubocurarine on action potentials in normal and denervated skeletal muscle. *J Physiol* **175**, 203–210.

Crofton HD (1971). Form, function and behavior. In *Plant Parasitic Nematodes*, ed. Zuckermann BM, Mai WF & Rohde RA, pp. 83–113. Academic Press, New York.

Cruz LJ, Gray WR, Olivera BM, Zeikus RD, Kerr L, Yoshikami D & Moczydlowski E (1985). *Conus geographus* toxins that discriminate between neuronal and muscle sodium channels. *J Biol Chem* **260**, 9280–9288.

Culetto E, Baylis HA, Richmond JE, Jones AK, Fleming JT, Squire MD *et al.* (2004). The *Caenorhabditis elegans* unc-63 gene encodes a levamisole-sensitive nicotinic acetylcholine receptor α subunit. *J Biol Chem* **279**, 42476–42483.

Davis MW, Fleischhauer R, Dent JA, Joho RH & Avery L (1999). A mutation in the *C. elegans* EXP-2 potassium channel that alters feeding behavior. *Science* **286**, 2501–2504.

de Bono M & Maricq AV (2005). Neuronal substrates of complex behaviors in *C. elegans*. *Annu Rev Neurosci* **28**, 451–501.

Dryer SE (2003). Molecular identification of the Na^+-activated K^+ channel. *Neuron* **37**, 727–728.

Evans TC (2006). Transformation and microinjection. In *WormBook*, ed. Wood WB & The *C. elegans* research community. http://www.wormbook.org.

Fawcett GL, Santi CM, Butler A, Harris T, Covarrubias M & Salkoff L (2006). Mutant analysis of the Shal (Kv4) voltage-gated fast transient K^+ channel in *Caenorhabditis elegans*. *J Biol Chem* **281**, 30725–30735.

Francis MM, Evans SP, Jensen M, Madsen DM, Mancuso J, Norman KR & Maricq AV (2005). The Ror receptor tyrosine kinase CAM-1 is required for ACR-16-mediated synaptic transmission at the *C. elegans* neuromuscular junction. *Neuron* **46**, 581–594.

Franks CJ, Pemberton D, Vinogradova I, Cook A, Walker RJ & Holden-Dye L (2002). Ionic basis of the resting membrane potential and action potential in the pharyngeal muscle of *Caenorhabditis elegans*. *J Neurophysiol* **87**, 954–961.

Hudson AJ, Ebers GC & Bulman DE (1995). The skeletal muscle sodium and chloride channel diseases. *Brain* **118**, 547–563.

Jentsch TJ, Friedrich T, Schriever A & Yamada H (1999). The CLC chloride channel family. *Pflugers Arch* **437**, 783–795.

Johnson CD & Stretton AOW (1980). Neural control of locomotion in *Ascaris*: anatomy, electrophysiology, and biochemistry. In *Nematodes as Biological Models*, ed. Zuckermann BM, pp. 159–195. Academic Press, New York.

Jospin M, Jacquemond V, Mariol MC, Segalat L & Allard B (2002). The L-type voltage-dependent Ca^{2+} channel EGL-19 controls body wall muscle function in *Caenorhabditis elegans*. *J Cell Biol* **159**, 337–348.

Jospin M, Watanabe S, Joshi D, Young S, Hamming K, Thacker C *et al*. (2007). UNC-80 and the NCA ion channels contribute to endocytosis defects in synaptojanin mutants. *Curr Biol* **17**, 1595–1600.

Kotlikoff MI (2003). Calcium-induced calcium release in smooth muscle: the case for loose coupling. *Prog Biophys Mol Biol* **83**, 171–191.

Kunkel MT, Johnstone DB, Thomas JH & Salkoff L (2000). Mutants of a temperature-sensitive two-P domain potassium channel. *J Neurosci* **20**, 7517–7524.

Kwok TC, Ricker N, Fraser R, Chan AW, Burns A, Stanley EF *et al*. (2006). A small-molecule screen in *C. elegans* yields a new calcium channel antagonist. *Nature* **441**, 91–95.

Lecroisey C, Segalat L & Gieseler K (2007). The *C. elegans* dense body: anchoring and signaling structure of the muscle. *J Muscle Res Cell Motil* **28**, 79–87.

Lee RY, Lobel L, Hengartner M, Horvitz HR & Avery L (1997). Mutations in the α1 subunit of an L-type voltage-activated Ca^{2+} channel cause myotonia in *Caenorhabditis elegans*. *EMBO J* **16**, 6066–6076.

Liu Q, Chen B, Gaier E, Joshi J & Wang ZW (2006). Low conductance gap junctions mediate specific electrical coupling in body-wall muscle cells of *Caenorhabditis elegans*. *J Biol Chem* **281**, 7881–7889.

Liu Q, Chen B, Yankova M, Morest DK, Maryon E, Hand AR *et al*. (2005). Presynaptic ryanodine receptors are required for normal quantal size at the *Caenorhabditis elegans* neuromuscular junction. *J Neurosci* **25**, 6745–6754.

Lockery SR & Goodman MB (2009). The quest for action potentials in *C. elegans* neurons hits a plateau. *Nat Neurosci* **12**, 377–378.

Lu B, Su Y, Das S, Liu J, Xia J & Ren D (2007). The neuronal channel NALCN contributes resting sodium permeability and is required for normal respiratory rhythm. *Cell* **129**, 371–383.

Maryon EB, Coronado R & Anderson P (1996). *unc-68* encodes a ryanodine receptor involved in regulating *C. elegans* body-wall muscle contraction. *J Cell Biol* **134**, 885–893.

Maryon EB, Saari B & Anderson P (1998). Muscle-specific functions of ryanodine receptor channels in *Caenorhabditis elegans*. *J Cell Sci* **111**, 2885–2895.

Mellem JE, Brockie PJ, Madsen DM & Maricq AV (2008). Action potentials contribute to neuronal signaling in *C. elegans*. *Nat Neurosci* **11**, 865–867.

Mitani A & Shattock MJ (1992). Role of Na-activated K channel, Na-K-Cl cotransport, and Na-K pump in $[K]_e$ changes during ischemia in rat heart. *Am J Physiol Heart Circ Physiol* **263**, H333–H340.

Moerman DG & Fire A (1997). Muscle: structure, function, and development. In *C elegans II*, ed. Riddle RL, Blumenthal T, Meyer BJ & Priess JR, pp. 417–470. Cold Spring Harbor Laboratory Press, Plainview.

Nakai J, Dirksen RT, Nguyen HT, Pessah IN, Beam KG & Allen PD (1996). Enhanced dihydropyridine receptor channel activity in the presence of ryanodine receptor. *Nature* **380**, 72–75.

Niebur E & Erdos P (1988). Computer simulation of networks of electrotonic neurons. In *Computer Simulation in Brain Science*, ed. Cotterill RMJ, pp. 148–163. Cambridge University Press, Cambridge.

Okkema PG, Harrison SW, Plunger V, Aryana A & Fire A (1993). Sequence requirements for myosin gene expression and regulation in *Caenorhabditis elegans*. *Genetics* **135**, 385–404.

Redfern P, Lundh H & Thesleff S (1970). Tetrodotoxin resistant action potentials in denervated rat skeletal muscle. *Eur J Pharmacol* **11**, 263–265.

Richmond JE & Jorgensen EM (1999). One GABA and two acetylcholine receptors function at the *C. elegans* neuromuscular junction. *Nat Neurosci* **2**, 791–797.

Richmond JE, Weimer RM & Jorgensen EM (2001). An open form of syntaxin bypasses the requirement for UNC-13 in vesicle priming. *Nature* **412**, 338–341.

Ruffin VA, Gu XQ, Zhou D, Douglas RM, Sun X, Trouth CO & Haddad GG (2008). The sodium-activated potassium channel Slack is modulated by hypercapnia and acidosis. *Neuroscience* **151**, 410–418.

Salkoff L (1985). Development of ion channels in the flight muscles of *Drosophila*. *J Physiol (Paris)* **80**, 275–282.

Salkoff L, Butler A, Fawcett G, Kunkel M, McArdle C, Paz-y-Mino G *et al*. (2001). Evolution tunes the excitability of individual neurons. *Neuroscience* **103**, 853–859.

Salkoff L, Wei AD, Baban B, Butler A, Fawcett G, Ferreira G & Santi CM (2005). Potassium channels in *C. elegans*. In *Wormbook*, ed. The *C. elegans* Research Community. http://www.wormbook.org.

Santi CM, Ferreira G, Yang B, Gazula VR, Butler A, Wei A *et al*. (2006). Opposite regulation of Slick and Slack K^+ channels by neuromodulators. *J Neurosci* **26**, 5059–5068.

Santi CM, Yuan A, Fawcett G, Wang ZW, Butler A, Nonet ML *et al*. (2003). Dissection of K^+ currents in *Caenorhabditis elegans* muscle cells by genetics and RNA interference. *Proc Natl Acad Sci U S A* **100**, 14391–14396.

Schneider MF (1994). Control of calcium release in functioning skeletal muscle fibers. *Annu Rev Physiol* **56**, 463–484.

Shtonda B & Avery L (2005). CCA-1, EGL-19 and EXP-2 currents shape action potentials in the *Caenorhabditis elegans* pharynx. *J Exp Biol* **208**, 2177–2190.

Steger KA, Shtonda BB, Thacker C, Snutch TP & Avery L (2005). The *C. elegans* T-type calcium channel CCA-1 boosts neuromuscular transmission. *J Exp Biol* **208**, 2191–2203.

Sulston JE & Hodgkin J (1988). Methods. In *The Nematode Caenorhabditis Elegans*, ed. Wood WB & The Community of *C. elegans* Researchers, pp. 587–606. Cold Spring Harbor Laboratory Press, Cold Spring Harbor, NY.

Tallini YN, Ohkura M, Choi BR, Ji G, Imoto K, Doran R *et al.* (2006). Imaging cellular signals in the heart *in vivo*: Cardiac expression of the high-signal Ca^{2+} indicator GCaMP2. *Proc Natl Acad Sci U S A* **103**, 4753–4758.

Tamsett TJ, Picchione KE & Bhattacharjee A (2009). NAD^{+} activates KNa channels in dorsal root ganglion neurons. *J Neurosci* **29**, 5127–5134.

Tanouye MA, Ferrus A & Fujita SC (1981). Abnormal action potentials associated with the *Shaker* complex locus of *Drosophila*. *Proc Natl Acad Sci U S A* **78**, 6548–6552.

Touroutine D, Fox RM, Von Stetina SE, Burdina A, Miller DM 3rd & Richmond JE (2005). *acr-16* encodes an essential subunit of the levamisole-resistant nicotinic receptor at the *Caenorhabditis elegans* neuromuscular junction. *J Biol Chem* **280**, 27013–27021.

Trimmer JS, Cooperman SS, Tomiko SA, Zhou JY, Crean SM, Boyle MB *et al.* (1989). Primary structure and functional expression of a mammalian skeletal muscle sodium channel. *Neuron* **3**, 33–49.

Tsien RW, Hess P, McCleskey EW & Rosenberg RL (1987). Calcium channels: mechanisms of selectivity, permeation, and block. *Annu Rev Biophys Biophys Chem* **16**, 265–290.

Verkhratsky A & Shmigol A (1996). Calcium-induced calcium release in neurones. *Cell Calcium* **19**, 1–14.

Wang ZW (2010). Origin of quantal size variation and high-frequency miniature postsynaptic currents at the *Caenorhabditis elegans* neuromuscular junction. *J Neurosci Res* **88**, 3425–3432.

Wang ZW, Saifee O, Nonet ML & Salkoff L (2001). SLO-1 potassium channels control quantal content of neurotransmitter release at the *C. elegans* neuromuscular junction. *Neuron* **32**, 867–881.

Wei A, Jegla T & Salkoff L (1996). Eight potassium channel families revealed by the *C. elegans* genome project. *Neuropharmacology* **35**, 805–829.

Wolters H, Wallinga W, Ypey DL & Boom HB (1994). Ionic currents during action potentials in mammalian skeletal muscle fibers analyzed with loose patch clamp. *Am J Physiol Cell Physiol* **267**, C1699–C1706.

Yeh E, Ng S, Zhang M, Bouhours M, Wang Y, Wang M *et al.* (2008). A putative cation channel, NCA-1, and a novel protein, UNC-80, transmit neuronal activity in *C. elegans*. *PLoS Biol* **6**, e55.

Yuan A, Dourado M, Butler A, Walton N, Wei A & Salkoff L (2000). SLO-2, a K^{+} channel with an unusual Cl^{-} dependence. *Nat Neurosci* **3**, 771–779.

Yuan A, Santi CM, Wei A, Wang ZW, Pollak K, Nonet M *et al.* (2003). The sodium-activated potassium channel is encoded by a member of the *Slo* gene family. *Neuron* **37**, 765–773.

Zhang L, Sukhareva M, Barker JL, Maric D, Hao Y, Chang YH *et al.* (2005). Direct binding of estradiol enhances Slack (sequence like a calcium-activated potassium channel) channels' activity. *Neuroscience* **131**, 275–282.

Author contributions

Conception and design: Z.-W.W., P.L. and B.C. Data collection and analysis: P.L. did all the electrophysiological and Ca^{2+} imaging experiments, and all data analysis. Q.G. first observed all-or-none action potentials in *C. elegans* body-wall muscle cells. B.C. made the transgenic strain expressing P*myo-3*::GCaMP2. Data interpretation: Z.-W.W., P.L., B.C., M.I.K. and L.S. Article drafting and revisions: Z.-W.W. with inputs from the coauthors. Experiments were done at University of Connecticut Health Center. All authors approved the final version of the manuscript.

Acknowledgements

This study was supported by National Institutes of Health (5R01GM083049 and 1R01MH085927 to Z.-W.W., 5RO1DK065992 and GM086736 to M.I.K., and R01NS0661871-01 to L.S.). The authors wish to thank Erik Jorgensen for the *unc-49* and *nca-1:nca-2* strains, Janet Richmond for the *unc-63:acr-16* strain, Ed Maryon for the *unc-68* strain, Caenorhabditis Genetic Center for the *unc-2, cca-1, egl-19, shl-1* and *shk-1* strains, and Xi Bie for building *slo-2:shk-1* double mutant and measuring solution osmolarities. The *nca-1, nca-2, shl-1* and *shk-1* strains were originally generated by the *C. elegans* Knockout Consortium.